Rapid Flow Assessment of Congenital Heart Disease with High-Spatiotemporal-Resolution Gated Spiral Phase-Contrast MR Imaging[1]

Jennifer A. Steeden, MEng
David Atkinson, PhD
Michael S. Hansen, PhD
Andrew M. Taylor, MD
Vivek Muthurangu, MD

Purpose: To validate a prospectively triggered spiral phase-contrast magnetic resonance (MR) sequence accelerated with sensitivity encoding (SENSE) in a population of children and adults with congenital heart disease.

Materials and Methods: The local research ethics committee approved this study, and written consent was obtained from all patients or guardians. Stroke volumes were quantified in 40 patients (mean age ± standard deviation: 21.4 years ± 13.8, age range: 3.0–61.3 years; 22 male patients aged 3.0–38.0 years [mean age, 17.2 years ± 10.5], 18 female patients aged 4.7–61.3 years [mean age, 26.6 years ± 15.9]) with congenital heart disease in the aorta (n = 40), main pulmonary artery (n = 38), right pulmonary artery (n = 22), and left pulmonary artery (n = 24). Stroke volumes were obtained with *(a)* breath-hold spiral phase-contrast MR imaging with SENSE, *(b)* conventional breath-hold cartesian phase-contrast MR imaging, and *(c)* reference free-breathing phase-contrast MR imaging. Stroke volumes were compared by using repeated-measures analysis of variance, Bland-Altman analysis, and correlation coefficients.

Results: Imaging time with the breath-hold spiral phase-contrast MR sequence was significantly lower than that with the conventional breath-hold phase-contrast MR sequence (~5 seconds vs ~16 seconds, respectively; $P < .0001$). There was excellent agreement in stroke volumes in all vessels between the reference free-breathing sequence (mean volume, 60.3 mL ± 27.3) and the two breath-hold sequences—spiral SENSE phase-contrast MR imaging (mean volume, 59.5 mL ± 27.1; $P < .001$) and conventional cartesian phase-contrast MR imaging (mean volume, 59.8 mL ± 27.6; $P = .268$). The limits of agreement were smaller with the spiral breath-hold sequence than with the conventional breath-hold sequence (−4.4 mL, 2.9 mL vs −10.3 mL, 9.3 mL, respectively); correlation was similar (r = 0.998 vs r = 0.984, respectively).

Conclusion: Flow volumes can be accurately and reliably quantified by using a spiral SENSE phase-contrast MR sequence, with high spatiotemporal resolution obtained in a short breath hold.

Supplemental material: *http://radiology.rsna.org/lookup/suppl/doi:10.1148/radiol.11101844/-/DC1*

[1] From the Centre for Medical Image Computing, UCL Department of Medical Physics & Bioengineering, London, England (J.A.S., D.A.); Centre for Cardiovascular MR, UCL Institute of Child Health, Great Ormond Street Hospital, Great Ormond St, London WC1N 3JH, England (J.A.S., M.S.H., A.M.T., V.M.); and National Institutes of Health, NHLBI, Bethesda, Md (M.S.H.). Supported by the Engineering and Physical Sciences Research Council. Received September 14, 2010; revision requested November 10; revision received December 8; accepted December 29; final version accepted January 25, 2011.
Address correspondence to V.M. (e-mail: *v.muthurangu@ich.ucl.ac.uk*).

Cardiac-gated phase-contrast magnetic resonance (MR) imaging is a proven method of measuring blood flow in the clinical environment (1–3). It is particularly useful in patients with congenital heart disease (4), where flow assessment often guides clinical decision making.

Phase-contrast MR imaging is intrinsically slow because each line in k-space must be acquired twice (with different velocity encodings) to perform background phase subtraction. Unfortunately, this prolongs acquisition time and prevents high-spatiotemporal-resolution phase-contrast MR imaging from being performed in a breath hold. Hence, gated phase-contrast MR imaging often relies on the acquisition of multiple signals to compensate for respiratory motion. This results in imaging times of approximately 2 minutes; thus, in congenital heart disease where four to eight separate flow measurements are often performed, complete flow assessment can take approximately 10 minutes. If spatiotemporal resolution is lowered, gated phase-contrast MR imaging can be performed in a breath hold (5). In children with congenital heart disease, however, high spatiotemporal resolution is necessary to assess smaller vessels at higher heart rates. Furthermore, the breath-hold times are often too long (>15 seconds) for children or sick adults. Thus, in the population with congenital heart disease there is a need for a high-spatiotemporal-resolution gated phase-contrast MR sequence that can be performed within a short breath hold.

One possible method of achieving this is to use efficient spiral trajectories. Furthermore, spiral trajectories can be combined with parallel imaging techniques, such as sensitivity encoding (SENSE), to further accelerate acquisition (6–9). With use of both these techniques, it is possible to perform phase-contrast MR imaging in real time (6,10–12). Unfortunately, real-time phase-contrast MR imaging comes at the cost of low spatiotemporal resolution and is not well suited to the pediatric population. Nevertheless, cardiac-gated spiral phase-contrast MR imaging, accelerated with parallel imaging, should provide the necessary high spatiotemporal resolution in a short breath hold.

We performed this study to validate a prospectively triggered spiral phase-contrast MR sequence accelerated with SENSE in a population of children and adults with congenital heart disease.

Advances in Knowledge

- High-spatiotemporal-resolution phase-contrast MR imaging can be achieved by using fast spiral trajectories and sensitivity-encoding (SENSE) acceleration.
- Breath-hold times with spiral SENSE phase-contrast MR imaging were significantly shorter than those with conventional cartesian phase-contrast MR imaging (~5 seconds vs ~16 seconds, respectively; $P < .0001$).
- Limits of agreement for measurement of stroke volumes, pulmonary-to-systemic flow ratios, and right-to-left pulmonary artery flow ratios were smaller with spiral breath-hold phase-contrast MR imaging than for conventional cartesian breath-hold phase-contrast MR imaging.

Materials and Methods

In July and August 2010, 40 consecutive children and adults (22 male and 18 female patients) referred for cardiac MR imaging were enrolled in this study. The mean patient age (±standard deviation) was 21.4 years ± 13.8 (range, 3.0–61.3 years). Seventeen patients were younger than 16 years. Fifteen patients had a repaired tetralogy of Fallot and/or pulmonary atresia with a ventricular septal defect, seven patients had coarctation of the aorta, six patients had cardiomyopathy, four patients had pulmonary stenosis, two patients had repaired transposition of the great arteries, two patients had secundum atrial septal defect, two patients had dilated aortic root, one patient had left pulmonary artery stenosis, and one patient had a bicuspid aortic valve. Five children were imaged while under general anesthesia.

The inclusion criterion was clinical referral for cardiac MR imaging. Pregnant patients or patients with MR imaging–incompatible implants were not referred for MR imaging. The exclusion criterion was an irregular heart rate (ie, multiple ectopic beats or atrial fibrillation; $n = 5$). The local research ethics committee approved the study, and written consent was obtained from all patients or guardians.

Imaging was performed with a 1.5-T MR unit (Avanto; Siemens Medical Solutions, Erlangen, Germany) by using two spine coils and one body matrix coil (giving a total of 12 coil elements). Flow was measured by using three sequences: *(a)* reference free-breathing phase-contrast MR imaging, *(b)* conventional

Implications for Patient Care

- In subjects who are unable to perform long breath holds, spiral SENSE phase-contrast MR imaging may be used to significantly decrease breath-hold time.
- Spiral SENSE phase-contrast MR imaging could significantly reduce total imaging time in patients with congenital heart disease without compromising accuracy of the flow assessment.

Published online before print
10.1148/radiol.11101844

Radiology 2011; 260:79–87

Abbreviations:
FOV = field of view
ROI = region of interest
SENSE = sensitivity encoding
SNR = signal-to-noise ratio
VNR = velocity-to-noise ratio

Author contributions:
Guarantors of integrity of entire study, J.A.S., V.K.; study concepts/study design or data acquisition or data analysis/interpretation, all authors; manuscript drafting or manuscript revision for important intellectual content, all authors; manuscript final version approval, all authors; literature research, J.A.S., M.S.H.; clinical studies, J.A.S., A.M.T., V.K.; statistical analysis, J.A.S., V.K.; and manuscript editing, all authors

Funding:
M.S.H. is an employee of the National Heart, Lung, and Blood Institute.

Potential conflicts of interest are listed at the end of this article.

breath-hold cartesian phase-contrast MR imaging, and *(c)* breath-hold spiral SENSE phase-contrast MR imaging. Imaging parameters are shown in Table 1. In addition, regurgitation was quantified where there was more than 10% regurgitant flow. A vector electrocardiographic system was used for cardiac gating.

Flow imaging was performed as per clinical need (vessels with stents were excluded) in the ascending aorta ($n = 40$, including four patients with regurgitation), main pulmonary artery ($n = 38$, including 12 patients with regurgitation), right pulmonary artery ($n = 22$, including 10 patients with regurgitation), and left pulmonary artery ($n = 24$, including 14 patients with regurgitation). Flow imaging was performed in both branch pulmonary vessels to assess differential blood flow and differential regurgitation fractions (13). Flow assessment was performed in each vessel by using the three sequences before moving to the next vessel.

The reference standard was a retrospectively gated, free-breathing, cartesian, gradient-echo phase-contrast MR sequence (provided by the manufacturer). Respiratory motion was compensated for by the acquisition of three signals. This sequence has high spatial and temporal resolution (Table 1) and is well-validated in vitro and in vivo (2,14–17); therefore, the flow volumes measured with this sequence were used as the reference standard.

The standard breath-hold sequence was a retrospectively gated, cartesian, phase-contrast MR sequence (provided by the manufacturer). This sequence was the same as the free-breathing flow sequence described earlier. However, the spatiotemporal resolution was lowered to acquire the data within a breath hold (Table 1).

The spiral sequence was a prospectively triggered, segmented, phase-contrast MR sequence developed in-house to enable high-spatiotemporal-resolution imaging in a short breath hold. A uniform-density spiral trajectory was used, with 36 spiral interleaves, undersampled by a factor of three (so only 12 spiral interleaves were acquired for each cardiac phase). Two spiral interleaves were acquired per R-R interval, meaning that six R-R intervals were used to acquire all of the data. One additional R-R interval was required at the beginning of imaging to reach a steady state. The sampling pattern was rotated for each cardiac phase so that three consecutive cardiac phases comprised a fully sampled k-space with 36 spiral readouts. These data were reconstructed online by using an iterative SENSE algorithm (18). The coil sensitivity information was calculated from the time-averaged (flow-compensated) data from each coil, divided by the sum of squares of the time-averaged coil data (12). The FOV was not optimized for children, as this would have resulted in a reduction in temporal resolution.

All images were processed by J.A.S. (with 3 years of experience in cardiovascular MR imaging) by using the open-source software OsiriX (OsiriX Foundation, Geneva, Switzerland) in a randomized order. For each flow measurement, the vessel of interest was segmented by using the modulus images. Segmentations were propagated by using a semiautomatic technique.

In the prospectively triggered spiral phase-contrast MR sequence, the acquisition window was automatically calculated from the average R-R interval, minus two times the standard deviation of the R-R interval. This meant that data in approximately the last 80 msec of diastole were not acquired. The missing flow data were predicted by performing a linear interpolation between the last calculated point and the first point, so that the flow profile filled the entire R-R interval (Appendix E1 [online]). It is important to estimate flow during the whole of diastole in patients with regurgitation or those in whom diastolic function is being assessed.

For each flow measurement, the stroke volume (net forward flow) and regurgitation fraction were calculated (by J.A.S.). In addition, where flow was measured in both the main pulmonary artery and ascending aorta ($n = 38$), the pulmonary-to-systemic flow ratio was calculated; where flow was measured in both the pulmonary branch vessels ($n = 20$), the ratio of right-to-left pulmonary artery flow was calculated (by J.A.S.) to assess the importance of any pulmonary artery branch stenosis.

In 10 randomly selected patients, the ascending aorta flow data obtained with all three sequences were re-analyzed

Table 1

Imaging Parameters

Parameter*	Free-Breathing Phase-Contrast MR Imaging	Conventional Breath-hold Phase-Contrast MR Imaging	Spiral Breath-hold Phase-Contrast MR Imaging
TR/TE (msec)	~7.0/2.2	~7.0/2.2	8.0/2.1
Spiral readouts	...	...	36
Acceleration factor	2 (GRAPPA)†	2 (GRAPPA)†	3 (SENSE)
Matrix size	256 × 192	192 × 113	256 × 256
FOV (mm)	200–400	290–400	400
Rectangular FOV (%)	75	66	100
Readouts per segment	3	4	2
Section thickness (mm)	5	5	5
Flip angle	30°	30°	25°
Pixel bandwidth (Hz/pixel)	543	543	1220
Velocity encoding (cm/sec)	180–400	180–400	180–400
No. of signals acquired	3	1	1
Total imaging time (sec)	44–144	11–24	3–8
Voxel size (mm)	0.8–1.5	1.5–2.1	1.6
Temporal resolution (msec)	~30.0	~40.0	32.0

* FOV = field of view, TE = echo time, TR = repetition time.

† GRAPPA = generalized autocalibrating partially parallel acquisition.

Figure 1

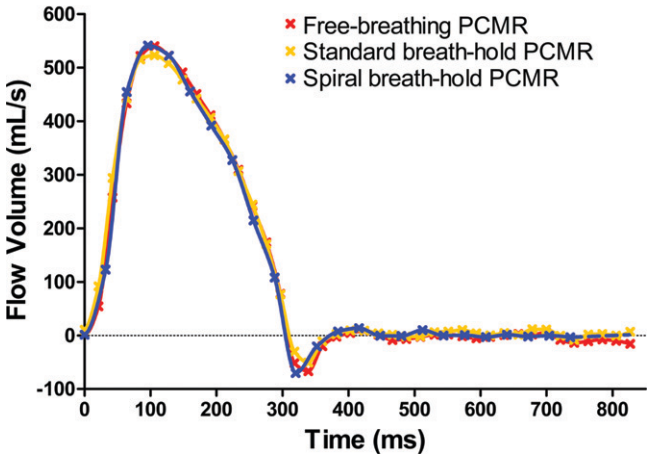

Figure 1: Comparison of flow profiles obtained with all three sequences in the ascending aorta of one patient. *PCMR* = phase-contrast MR imaging.

(by J.A.S.) to determine intraobserver variability. These data were also analyzed by a second operator (V.M., with 8 years of experience in cardiovascular MR imaging) to determine interobserver variability.

Image quality was assessed in all vessels (ascending aorta, $n = 40$; main pulmonary artery, $n = 38$; right pulmonary artery, $n = 22$; left pulmonary artery, $n = 24$; total vessels, $n = 124$) for all three sequences by using measures of signal-to-noise ratio (SNR), velocity-to-noise ratio (VNR), and edge sharpness (by J.A.S.). All image quality analyses were carried out by using in-house plug-ins for OsiriX.

True quantification of SNR and VNR in images acquired with noncartesian parallel imaging is nontrivial in the clinical environment owing to the uneven distribution of noise (19–21). Therefore, in this study, estimated SNR (σ_S) and VNR (σ_V) were calculated in the same way as in previous studies (21,22). In summary, a region of interest (ROI) was drawn in stationary tissue, and estimated noise was calculated as the average standard deviation of the pixel intensity (σ_S) or velocity (σ_V) through all cardiac phases. σ_S was calculated in all images after correcting for exponential signal decay, from a nonsteady state. Final estimates of SNR were made from the corrected mean signal intensity and final estimates of VNR from the mean velocity, within an ROI drawn in the vessel during peak systole, divided by σ_S and σ_V, respectively.

A quantitative edge sharpness value was calculated in all vessels ($n = 124$) by measuring the maximum gradient of the normalized pixel intensities across the border of the volume of interest (20,22). To reduce noise, which results in artificially high gradients (representing sharp edges), the pixel intensities were filtered by using a Savitzky-Golay filter (23) (window width, 6 pixels; third-order polynomial) before differentiation. Edge sharpness was calculated for all cardiac phases, and the average value was used for comparison.

The sample size was chosen to detect a mean difference in stroke volumes of 2.0 mL (mean and standard deviation assumed from literature values [5]), with a statistical power of 80% and a P value of .05. This value was chosen because it was believed to be the lowest clinically significant deviation. This analysis was performed by using open-source software (G*power 3; University of Dusseldorf, Dusseldorf, Germany) (24), which gave an estimated sample size of 36 (which was increased to 40 for this study). All statistical analyses were performed by using software (Prism; GraphPad Software, San Diego, Calif). The results were combined for all patients and are expressed as means ± standard deviations. Comparison of means was performed by using repeated-measures analysis of variance, with Bonferroni correction for multiple comparisons. $P < .05$ was indicative of a statistically significant difference. Bland-Altman analysis was performed to give measures of agreement with the free-breathing phase-contrast MR sequence (25). In addition, correlation coefficients were calculated.

Results

The average heart rate was 76 beats per minute ± 12 (range, 50–111 beats per minute). For the reference free-breathing sequence, data were acquired over 108 heartbeats (mean, 91 seconds ± 17; range, 44–144 seconds). In the standard breath-hold sequence, data were acquired over 18 heartbeats (mean, 16 seconds ± 3; range, 11–24 seconds). For the spiral breath-hold sequence, data were acquired over seven heartbeats (mean, 5 seconds ± 1; range, 3–8 seconds).

Good agreement was seen throughout the cardiac cycle for all sequences, as can be seen in Figure 1. When evaluating all vessels combined ($n = 124$), there were no significant differences in mean stroke volume calculated with the reference free-breathing sequence (60.3 mL ± 27.3), standard breath-hold sequence (59.8 mL ± 27.6), and spiral breath-hold sequence (59.5 mL ± 27.1). Results of Bland-Altman analysis comparing the breath-hold sequences to the reference free-breathing sequence are shown in Figure 2. There was no clinically significant bias with either breath-hold sequence (spiral breath-hold phase-contrast MR imaging: −0.7 mL; standard breath-hold phase-contrast MR imaging: −0.5 mL). However, the limits of agreement and correlation for the spiral breath-hold sequence were smaller than and similar to, respectively, those with the conventional breath-hold sequence (−4.4 mL, 2.9 mL vs −10.3 mL, 9.3 mL, respectively; $r = 0.998$ vs $r = 0.984$, respectively).

Results of Bland-Altman analyses and correlations performed separately for the ascending aorta, main pulmonary artery, and branch pulmonary arteries are shown in Table 2. There were no statistically significant differences in stroke volumes calculated with any of the

Radiology

Figure 2

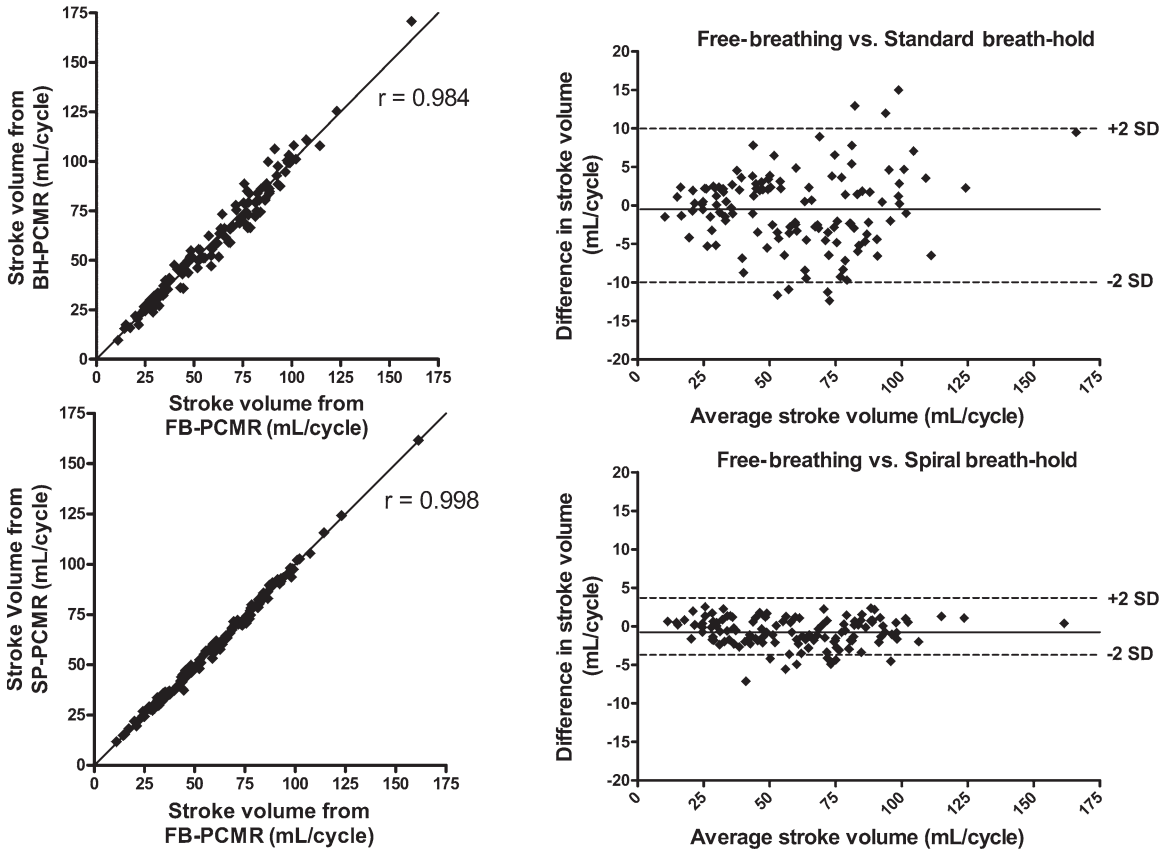

Figure 2: Comparisons of stroke volumes obtained in all vessels with free-breathing phase-contrast MR imaging (*FB-PCMR*) versus conventional breath-hold phase-contrast MR imaging (*BH-PCMR*) (top) and with free-breathing phase-contrast MR imaging versus spiral breath-hold phase-contrast MR imaging (*SP-PCMR*) (bottom). Scatterplots are shown on left, and corresponding Bland-Altman plots are on right. *SD* = standard deviation.

sequences. At Bland-Altman analysis, we found only a small bias in stroke volume between the free-breathing sequence and both breath-hold sequences (spiral breath-hold vs conventional breath-hold, respectively: ascending aorta, −0.9 mL vs −1.3 mL; main pulmonary artery, −0.8 mL vs −0.5 mL; pulmonary branches: −0.6 mL vs 0.2 mL). For all vessels, limits of agreement with spiral breath-hold acquisition were smaller and correlation was greater than those with conventional breath-hold acquisition (limits of agreement: ascending aorta = −4.6 mL, 2.8 mL vs −11.1 mL, 8.5 mL, respectively, main pulmonary artery = −4.4 mL, 2.8 mL vs −13.1 mL, 12.1 mL, pulmonary branches = −4.2 mL, 3.1 mL vs −6.5 mL, 6.8 mL; correlation coefficients: ascending aorta = 0.996 vs 0.968, respectively, main pulmonary artery = 0.998 vs 0.976, pulmonary branches = 0.995 vs 0.985).

In this study, 21 vessels were imaged in seven patients with heart rates faster than 90 beats per minute (ascending aorta, n = 7; main pulmonary artery, n = 7; right pulmonary artery, n = 4; left pulmonary artery, n = 3). Bland-Altman analysis of these stroke volumes found a small bias between the free-breathing sequence and both breath-hold sequences (conventional breath-hold sequence, −0.78 mL; spiral breath-hold sequence, −0.53 mL). In these vessels, the limits of agreement were smaller for the spiral breath-hold acquisition than for the standard breath-hold acquisition (−3.70 mL, 2.64 mL vs −8.31 mL, 6.76 mL, respectively).

Forty-seven vessels were less than 2.0 cm in diameter (ascending aorta, n = 6; main pulmonary artery, n = 7; right pulmonary artery, n = 16; left pulmonary artery, n = 18). Bland-Altman analysis of the stroke volumes in these vessels found a small bias between the free-breathing sequence and both breath-hold sequences (conventional breath-hold sequence, 0.14 mL; spiral breath-hold sequence, −0.48 mL). The limits of agreement for these vessels were smaller for spiral breath-hold acquisition than for conventional breath-hold acquisition (−3.97 mL, 3.00 mL vs −6.91 mL, 7.19 mL, respectively). Because of the insufficient number of vessels with these characteristics, we did not calculate pulmonary-to-systemic flow and right-to-left pulmonary artery flow ratios.

Regurgitant flow was found in 40 vessels (Table 3). There was no significant difference in the regurgitation fractions seen with free-breathing versus conventional breath-hold phase-contrast MR imaging. However, a small but statistically significant difference (−2.0%) was found between regurgitation fractions seen with free-breathing versus spiral breath-hold phase-contrast MR sequences. Despite this finding, the correlation coefficient was found to be higher and limits of agreement were found to be lower with the spiral breath-hold acquisition compared with the standard breath-hold acquisition (r = 0.986 vs 0.971, respectively; limits of agreement = −6.8%, 2.8% vs −8.2%, 5.9%, respectively).

Pulmonary-to-systemic flow and right-to-left pulmonary artery flow ratios were calculated where possible (Table 3). No significant differences were found between any of the sequences. Bland-Altman analysis found the limits of agreement were smaller and the correlation was greater with the spiral breath-hold acquisition than with the standard breath-hold acquisition (pulmonary-to-systemic flow ratio: limits of agreement = −0.08, 0.10 vs −0.23, 0.27, r = 0.989 vs 0.933, respectively; right-to-left pulmonary artery flow ratio: limits of agreement = −0.22, 0.12 vs −0.32, 0.21, r = 0.991 vs 0.973, respectively).

For 10 randomly selected subjects, the ascending aorta data from all three sequences were re-evaluated by the same observer (J.A.S.). The mean difference in stroke volumes was 0.5% ± 1.2 (range, −1.1% to 2.9%; P = .25) for the free-breathing sequence, 0.9% ± 2.4 (range, −3.6% to 5.6%; P = .20) for the conventional breath-hold sequence, and −0.3% ± 1.2 (range, −2.6% to 1.6%; P = .22) for the spiral breath-hold sequence. There were no statistically significant differences between the repeated measures for any of the sequences.

These data sets were also independently reviewed by a second observer (V.M.) to assess interobserver variability. The mean difference in stroke volumes was 0.1% ± 1.5 (range, −2.5% to 3.4%; P = .75) for the free-breathing sequence, 0.7% ± 2.3 (range, −3.9% to 3.6%; P = .40) for the conventional

Table 2

Comparison of Stroke Volumes Calculated with the Three Sequences

Parameter	Free-Breathing Phase-Contrast MR Imaging	Conventional Breath-hold Phase-Contrast MR Imaging	Spiral Breath-hold Phase-Contrast MR Imaging
Aorta			
Mean stroke volume (mL)	68.6 ± 19.6	67.3 ± 19.6	67.7 ± 19.9
Bias (mL)*†	...	−1.3 (−2.89, 0.30)	−0.9 (−1.52, −0.31)
Limits of agreement (mL)†	...	−11.1, 8.5	−4.6, 2.8
Correlation coefficient†	...	0.968	0.996
Main pulmonary artery			
Mean stroke volume (mL)	76.6 ± 27.6	76.2 ± 29.1	75.9 ± 27.7
Bias (mL)*†	...	−0.5 (−2.59, 1.63)	−0.8 (−1.37, −0.16)
Limits of agreement (mL)†	...	−13.1, 12.1	−4.4, 2.8
Correlation coefficient†	...	0.976	0.998
Pulmonary branches			
Mean stroke volume (mL)	39.5 ± 18.5	39.7 ± 19.2	38.9 ± 18.1
Bias (mL)*†	...	0.2 (−0.82, 1.19)	−0.6 (−1.11, 0.00)
Limits of agreement (mL)†	...	−6.5, 6.8	−4.2, 3.1
Correlation coefficient†	...	0.985	0.995

* Numbers in parentheses are 95% confidence intervals.

† Compared with the free-breathing phase-contrast MR sequence.

Table 3

Regurgitation Fraction, Pulmonary-to-Systemic Flow Ratio, and Right-to-Left Pulmonary Artery Flow Ratio Calculated with the Three Sequences

Parameter	Free-Breathing Phase-Contrast MR Imaging	Conventional Breath-hold Phase-Contrast MR Imaging	Spiral Breath-hold Phase-Contrast MR Imaging
Regurgitation (n = 40)			
Mean regurgitation fraction (%)	31.1 ± 14.7	30.0 ± 15.0	29.1 ± 14.2*
Range (%)	11.16–60.8	6.4–60.4	8.6–55.7
Bias (%)†‡	...	−1.1 (−2.28, 0.02)	−2.0 (−2.82, −1.25)
Limits of agreement (%)†	...	−8.2, 5.9	−6.8, 2.8
Correlation coefficient†	...	0.971	0.986
Q_p/Q_s (n = 38)§			
Mean Q_p/Q_s	1.13 ± 0.29	1.15 ± 0.34	1.14 ± 0.30
Range	0.81–2.64	0.78–2.92	0.83–2.73
Bias†‡	...	0.018 (−0.02, 0.06)	0.006 (−0.01, 0.02)
Limits of agreement†	...	−0.23, 0.27	−0.08, 0.10
Correlation coefficient†	...	0.933	0.989
RPA/LPA (n = 20)‖			
Mean RPA/LPA	1.44 ± 0.59	1.42 ± 0.65	1.39 ± 0.53
Range	0.55–2.78	0.44–2.62	0.54–2.70
Bias†‡	...	−0.049 (−0.11, 0.01)	−0.050 (−0.09, −0.01)
Limits of agreement†	...	−0.32, 0.21	−0.22, 0.12
Correlation coefficient†	...	0.973	0.991

* Value is significantly different from that with the free-breathing phase-contrast MR sequence (P < .05).

† Compared with the free-breathing phase-contrast sequence.

‡ Numbers in parentheses are 95% confidence intervals.

§ Q_p/Q_s = pulmonary-to-systemic flow ratio.

‖ RPA/LPA = right-to-left pulmonary artery flow ratio.

Figure 3

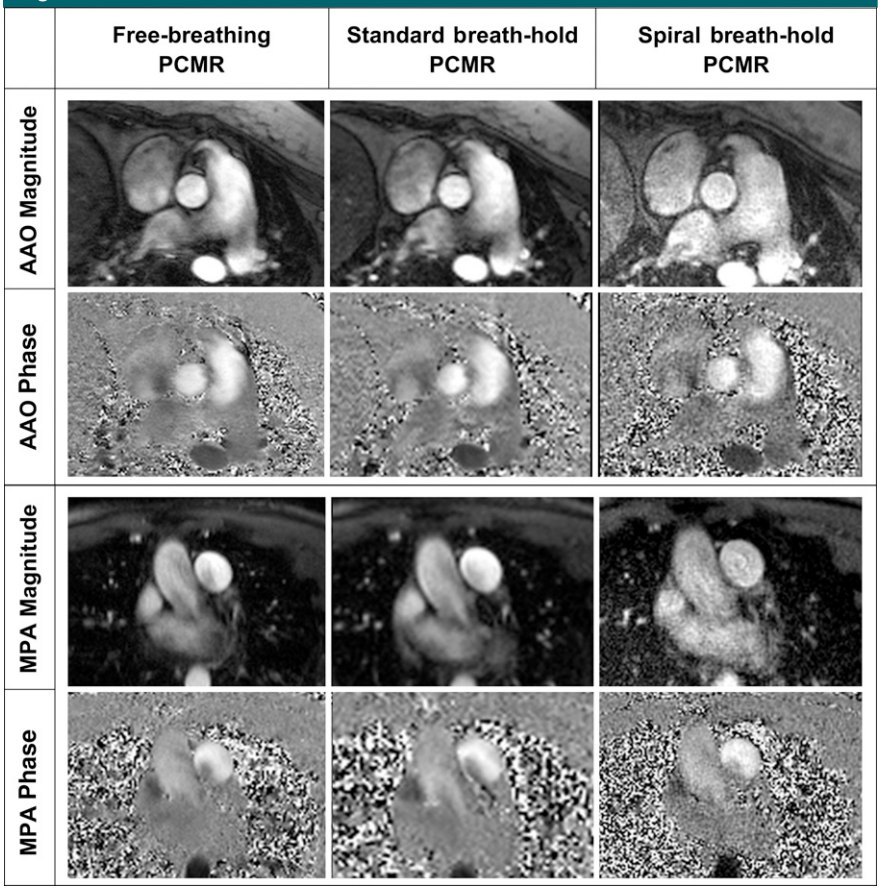

Figure 3: Examples of image quality obtained with the three sequences in the ascending aorta (*AAO*) and main pulmonary artery (*MPA*). *PCMR* = phase-contrast MR imaging.

Table 4

Summary of Image Quality Metrics

Parameter	Free-Breathing Phase-Contrast MR Imaging	Conventional Breath-hold Phase-Contrast MR Imaging	Spiral Breath-hold Phase-Contrast MR Imaging
Estimated signal variation or σ_S	5.4 ± 1.4	5.9 ± 1.5*	8.6 ± 2.2*†
Stationary σ_S/free-breathing σ_S	...	1.1 ± 0.3	1.7 ± 0.6
Estimated SNR	45.6 ± 14.9	41.7 ± 14.2*	31.9 ± 11.6*†
Estimated velocity variation or σ_V (cm/sec)	17.6 ± 9.1	19.5 ± 10.5*	19.7 ± 7.7*
Stationary σ_V/free-breathing σ_V	...	1.1 ± 04	1.2 ± 0.4
Estimated VNR	8.4 ± 4.8	7.4 ± 3.9*	6.7 ± 3.1*†
Edge sharpness (mm^{-1})	0.78 ± 0.36	0.74 ± 0.34	0.78 ± 0.35

* Value is significantly different from that at free-breathing phase-contrast MR imaging ($P < .05$).

† Value is significantly different from that at conventional breath-hold phase-contrast MR imaging ($P < .05$).

breath-hold sequence, and −0.5% ± 1.5 (range, −2.7% to 2.5%; $P = .21$) for the spiral breath-hold sequence. There were no statistically significant differences between the repeated measures for any of the sequences.

Figure 3 shows examples of the image quality from all three tested sequences in the ascending aorta and main pulmonary artery. Quantitative image quality metrics can be seen in Table 4.

The estimated SNR and VNR obtained with the free-breathing phase-contrast MR sequence were higher than those with both of the breath-hold phase-contrast MR sequences ($P < .05$). The estimated SNRs and VNRs with spiral breath-hold phase-contrast MR imaging were lower than those with free-breathing and conventional breath-hold phase-contrast MR imaging ($P < .05$).

Edge sharpness was not significantly different among any of the sequences (Table 4). However, the free-breathing phase-contrast MR images and the spiral breath-hold phase-contrast MR images had the same average edge sharpness; edge sharpness was slightly lower with the standard breath-hold phase-contrast MR images.

Discussion

We have demonstrated that is it possible to use a prospectively triggered, undersampled, spiral phase-contrast MR sequence with a SENSE reconstruction algorithm to accurately and reliably measure flow within a short breath hold. Currently, high-spatiotemporal-resolution, free-breathing, cardiac-gated phase-contrast MR imaging is used as the reference standard for the measurement of flow in patients with congenital heart disease. Unfortunately, owing to multiple signal acquisitions, each flow assessment can take more than 2 minutes to perform. Thus, in MR imaging of congenital heart disease, where four to eight separate flow assessments are necessary, flow imaging can take up a substantial proportion of the total imaging time. The spiral breath-hold sequence used in this study should enable reduction of the total duration of flow imaging from an average of 10 minutes to less than 1 minute. This would lead to a marked reduction in total imaging time and has implications for patient throughput and compliance for cardiac MR imaging of patients with congenital heart disease.

Achieving high-spatiotemporal-resolution phase-contrast MR imaging in a

short breath hold requires efficient filling of k-space. In this study, spiral trajectories were used to significantly reduce the acquisition time. Imaging was further accelerated with noncartesian SENSE. The resultant sequence had a breath-hold time of ~5 seconds, compared with ~16 seconds for the conventional cartesian breath-hold phase-contrast MR sequence. Furthermore, unlike the standard breath-hold sequence, spatiotemporal resolution was not compromised to achieve the short breath hold. This makes this spiral sequence useful in both children and sick adults who are unable to perform long breath holds. In this study, most of our patients were adolescents or adults, as this represents the population seen in most MR examinations of congenital heart disease. There are some disadvantages to spiral trajectories and parallel imaging, including off-resonance effects and trajectory errors as well as a reduced SNR. However, these were not seen to affect the accuracy of the spiral phase-contrast MR sequence in this study.

For stroke volumes and pulmonary-to-systemic and right-to-left pulmonary artery flow ratios, there was excellent agreement between the spiral breath-hold sequence and the reference free-breathing sequence. Furthermore, the spiral breath-hold sequence was found to give smaller limits of agreement and higher correlation compared with the conventional breath-hold sequence. This is most likely owing to the higher temporal and spatial resolution of the spiral breath-hold sequence. It may also be attributed to the shorter breath-hold times, which may prevent residual breathing as well as limit heart rate variability during imaging. In addition, the intra- and interobserver variability seen with the spiral breath-hold phase-contrast MR sequence was good.

There was, however, a small but statistically significant difference in the regurgitation fractions calculated with the free-breathing phase-contrast MR sequence and the spiral breath-hold sequence. This was probably due to the interpolation of the flow curve at the very end of diastole in the prospectively triggered spiral sequence. It should be noted, however, that the difference in regurgitation fraction was on average only 2%, which would not be considered clinically important.

The edge sharpness with the spiral breath-hold sequence was similar to that with the free-breathing sequence and higher than that with the conventional breath-hold sequence. This is most likely due to the lower spatial resolution of the conventional breath-hold phase-contrast MR sequence. The good edge sharpness with the spiral breath-hold sequence may have benefits in terms of either manual or automatic segmentation of the vessels compared with standard breath-hold sequences.

The estimated SNR and VNR, however, were lower with the spiral breath-hold sequence than with the free-breathing and conventional breath-hold sequences. This is due to *(a)* the higher acceleration factor used with the spiral breath-hold sequence compared with the other two sequences, *(b)* the much higher bandwidth used with the spiral breath-hold sequence compared with the other two sequences, *(c)* the fact that multiple signals were not acquired with the spiral breath-hold sequence (unlike the free-breathing phase-contrast MR sequence), and *(d)* the higher spatial resolution with the spiral breath-hold sequence compared with the conventional breath-hold sequence.

The main limitation of using an undersampled spiral trajectory is the need for a large FOV to prevent wrapping of signal and to ensure accurate reconstruction of the undersampled data. Because we do not use a selective excitation, it is necessary for the FOV to be larger than the object being imaged. In the future, the FOV could be reduced by using improved coil configurations or radiofrequency shielding of the arms and torso. In addition, a spatially selective radiofrequency pulse or saturation bands could be used; however, these would increase the imaging time or reduce the temporal resolution.

As seen from the results of image quality analysis, the SNR and VNR with the spiral breath-hold phase-contrast MR sequence were significantly lower than those with either the conventional breath-hold phase-contrast MR sequence or the free-breathing sequence. Although this is a limitation of the sequence, it did not affect the accuracy of the stroke volume measurements obtained in this study.

Currently, MR flow assessment can take more than 10 minutes in patients with congenital heart disease owing to the need to measure flow in four to eight vessels. Thus, it often represents almost 25% of total imaging time. With use of the spiral breath-hold sequence validated in this study, all flow imaging could be performed in less than 1 minute. This would significantly reduce total imaging time without compromising the accuracy of the flow assessment. The benefits of this would be twofold. First, in the pediatric population a shorter total imaging time would be less demanding on the patients and improve compliance. Second, shorter imaging times should improve patient throughput. Therefore, we believe that this sequence has substantial benefits in MR imaging of congenital heart disease.

Disclosures of Potential Conflicts of Interest: **J.A.S.** Financial activities related to the present article: none to disclose. Financial activities not related to the present article: none to disclose. Other relationships: none to disclose. **D.A.** Financial activities related to the present article: none to disclose. Financial activities not related to the present article: institution received a grant or grants are pending from Siemens Healthcare. Other relationships: none to disclose. **M.S.H.** Financial activities related to the present article: none to disclose. Financial activities not related to the present article: none to disclose. Other relationships: none to disclose. **A.M.T.** Financial activities related to the present article: received a grant from Siemens Medical Solutions. Financial activities not related to the present article: none to disclose. Other relationships: none to disclose. **V.M.** Financial activities related to the present article: none to disclose. Financial activities not related to the present article: received payment for lectures including service on speakers bureaus from Medtronic. Other relationships: none to disclose.

References

1. Firmin DN, Nayler GL, Klipstein RH, Underwood SR, Rees RSO, Longmore DB. In vivo validation of MR velocity imaging. J Comput Assist Tomogr 1987;11(5):751–756.

2. Beerbaum P, Körperich H, Barth P, Esdorn H, Gieseke J, Meyer H. Noninvasive quantification of left-to-right shunt in pediatric patients:

phase-contrast cine magnetic resonance imaging compared with invasive oximetry. Circulation 2001;103(20):2476–2482.

3. Van Rossum AC, Sprenger M, Visser FC, Peels KH, Valk J, Roos JP. An in vivo validation of quantitative blood flow imaging in arteries and veins using magnetic resonance phase-shift techniques. Eur Heart J 1991;12(2):117–126.

4. Rees S, Firmin D, Mohiaddin R, Underwood R, Longmore D. Application of flow measurements by magnetic resonance velocity mapping to congenital heart disease. Am J Cardiol 1989;64(14):953–956.

5. Sakuma H, Kawada N, Kubo H, et al. Effect of breath holding on blood flow measurement using fast velocity encoded cine MRI. Magn Reson Med 2001;45(2):346–348.

6. Steeden JA, Atkinson D, Taylor AM, Muthurangu V. Assessing vascular response to exercise using a combination of real-time spiral phase contrast MR and noninvasive blood pressure measurements. J Magn Reson Imaging 2010;31(4):997–1003.

7. Nezafat R, Kellman P, Derbyshire JA, McVeigh ER. Real-time blood flow imaging using autocalibrated spiral sensitivity encoding. Magn Reson Med 2005;54(6):1557–1561.

8. Nayak KS, Pauly JM, Kerr AB, Hu BS, Nishimura DG. Real-time color flow MRI. Magn Reson Med 2000;43(2):251–258.

9. Qian Y, Zhang Z, Stenger VA, Wang Y. Self-calibrated spiral SENSE. Magn Reson Med 2004;52(3):688–692.

10. Gatehouse PD, Firmin DN, Collins S, Longmore DB. Real time blood flow imaging by spiral scan phase velocity mapping. Magn Reson Med 1994;31(5):504–512.

11. Körperich H, Gieseke J, Barth P, et al. Flow volume and shunt quantification in pediatric congenital heart disease by real-time magnetic resonance velocity mapping: a validation study. Circulation 2004;109(16):1987–1993.

12. Nezafat R, Kellman P, Derbyshire JA, McVeigh ER. Real time high spatial-temporal resolution flow imaging with spiral MRI using auto-calibrated SENSE. In: Proceedings of the 26th Annual International Conference of the Engineering in Medicine and Biology Society. Piscataway, NJ: IEEE Engineering in Medicine and Biology Society, 2004;1:1914–1917.

13. Kang IS, Redington AN, Benson LN, et al. Differential regurgitation in branch pulmonary arteries after repair of tetralogy of Fallot: a phase-contrast cine magnetic resonance study. Circulation 2003;107(23):2938–2943.

14. Powell AJ, Maier SE, Chung T, Geva T. Phase-velocity cine magnetic resonance imaging measurement of pulsatile blood flow in children and young adults: in vitro and in vivo validation. Pediatr Cardiol 2000;21(2):104–110.

15. Evans AJ, Iwai F, Grist TA, et al. Magnetic resonance imaging of blood flow with a phase subtraction technique: in vitro and in vivo validation. Invest Radiol 1993;28(2):109–115.

16. Frayne R, Steinman DA, Ethier CR, Rutt BK. Accuracy of MR phase contrast velocity measurements for unsteady flow. J Magn Reson Imaging 1995;5(4):428–431.

17. Meier D, Maier S, Bösiger P. Quantitative flow measurements on phantoms and on blood vessels with MR. Magn Reson Med 1988;8(1):25–34.

18. Pruessmann KP, Weiger M, Börnert P, Boesiger P. Advances in sensitivity encoding with arbitrary k-space trajectories. Magn Reson Med 2001;46(4):638–651.

19. Dietrich O, Raya JG, Reeder SB, Reiser MF, Schoenberg SO. Measurement of signal-to-noise ratios in MR images: influence of multichannel coils, parallel imaging, and reconstruction filters. J Magn Reson Imaging 2007;26(2):375–385.

20. Muthurangu V, Lurz P, Critchely JD, Deanfield JE, Taylor AM, Hansen MS. Real-time assessment of right and left ventricular volumes and function in patients with congenital heart disease by using high spatiotemporal resolution radial k-t SENSE. Radiology 2008;248(3):782–791.

21. Nielsen JF, Nayak KS. Referenceless phase velocity mapping using balanced SSFP. Magn Reson Med 2009;61(5):1096–1102.

22. Steeden JA, Atkinson D, Taylor AM, Muthurangu V. Split-acquisition real-time CINE phase-contrast MR flow measurements. Magn Reson Med 2010;64(6):1664–1670.

23. Savitzky A, Golay MJ. Smoothing and differentiation of data by simplified least squares procedures. Anal Chem 1964;36(8):1627–1639.

24. Faul F, Erdfelder E, Lang A-G, Buchner AG. G*Power 3: a flexible statistical power analysis program for the social, behavioral, and biomedical sciences. Behav Res Methods 2007;39(2):175–191.

25. Bland JM, Altman DG. Statistical methods for assessing agreement between two methods of clinical measurement. Lancet 1986;1(8476):307–310.